

The genus *Parapseudomma* from the East Atlantic deep sea, with description of a new species (Mysida: Mysidae)

Karl J. Wittmann 

Medical University of Vienna, Department of Environmental Health, Vienna, Austria.

KJW E-mail: karl.wittmann@meduniwien.ac.at

ZOOBANK: <https://zoobank.org/urn:lsid:zoobank.org:pub:8B0850D1-1A18-4199-89D9-331FF94BBC13>

ABSTRACT

Revised diagnoses are given for the mysid genus *Parapseudomma* Nouvel and Lagardère, 1976, and its type species *Parapseudomma calloplura* (Holt and Tattersall, 1905) from the Northeast-Atlantic, Mediterranean and waters off Japan, depth range 94–1200 m. *Parapseudomma stenurum* n. sp. from the sea floor off Cape Verde Islands and the Angola Basin, depth range 3825–5460 m, is described as the second species of its genus. It differs from the type species mainly by an unsegmented antennal scale, the carpus of thoracic endopods 3–8 separated from the propodus by a transverse articulation, the digitus mobilis of the right mandible reduced to a slender spine, and by a more slender telson. Reduction of the right digitus is also found in *Abyssomysis* and *Xenomysis*, the latter with potential genetic affinity to *Parapseudomma*. The three genera also share reduced eyes as in many other deep-sea Erythropinae. Both species of *Parapseudomma* share recently detected, probably sensorial structures: a pit-like depression here named ‘antennular bursa’, dorsally on the basal segment of the antennula, and a median ‘eye-cyst’ inside the fused ‘eye-bar’, the cyst opening to the surface by a duct. The evidence in *Parapseudomma* raises expectations that these sensorial organs are potentially present in a great variety of Erythropinae taxa.

KEYWORDS

Abyssobenthic, morphology, new species, revision, taxonomy, sensorial structures

Editor-in-chief
Christopher Tudge

Associate Editor:
Shane Ahyong

Corresponding Author
Karl Wittmann
karl.wittmann@meduniwien.ac.at

Submitted 03 October 2022
Accepted 03 January 2023
Published 18 August 2023

DOI 10.1590/2358-2936e2023013



All content of the journal, except where identified, is licensed under a Creative Commons attribution-type BY.

Nauplius, 31:e2023013

INTRODUCTION

Among 171 currently (29 Sep 2022) acknowledged Recent genera in the family Mysidae, the previously monotypic genus *Parapseudomma* Nouvel and Lagardère, 1976, shows the greatest similarity with the species-rich *Pseudomma* G.O. Sars, 1870. In retrospective view it was hidden for seven decades in the shadows of the latter genus as *Pseudomma calloplura* Holt and Tattersall, 1905. Already at its first description in 1905, Holt and Tattersall expressed some doubts on the affiliation of this species and finally decided to include it in the genus *Pseudomma* based on the highly similar structure of the eye rudiment. As late as 1976, Nouvel and Lagardère upgraded it to genus level as *Parapseudomma* by claiming that it cannot remain in the genus *Pseudomma* due to a two-segmented antennal scale, terminal margin of the telson with minute median spine flanked by large rugged spines, telson without setae, short rostral process of the labrum, modified seta arising from the penultimate segment of the endopod of pleopod 4 in adult males, and thoracic sternal processes in non-adults of both sexes. As many as 34 currently acknowledged species of *Pseudomma* were described up to 1976, thereafter fewer, yielding a total of 46 species. Both counts include the poorly known *Pseudomma oculospinum* W.M. Tattersall, 1951 (syn. *Scolamblyops oculospinum* emend. Murano, 1974) based on eye morphology; not acknowledged by Wittmann et al. (2014) as pertaining to the genus *Scolamblyops* Murano, 1974. Due to the comparatively great number of species, it is unsurprising that most of the individual characters claimed by Nouvel and Lagardère (1976) (unlike certain combinations of characters) are actually shared by one or more species of *Pseudomma*. Only the process of the labrum and the sternal processes in non-adults remain as autapomorphic characters of *Parapseudomma* (for additional characters see below), with the reservation that the respective characters are insufficiently known in many species of *Pseudomma*. Nonetheless, Kou et al. (2020) depicted *Parapseudomma* and *Pseudomma* in different clusters based on molecular phylogenetic analysis, though based on only a few species.

A single specimen of *Parapseudomma* with unusually slender telson is identified in the present contribution based on materials taken in 1982 by the CANCAP-VI expedition to the deep sea off Cape Verde Islands (equatorial NE-Atlantic). The structure of the telson is reminiscent of mysids taken in 2000 by the DIVA-1 expedition to the deep sea floor of the Angola Basin (equatorial SE-Atlantic) and determined by Wittmann (2020) as *Parapseudomma calloplura* (Holt and Tattersall, 1905). Hence the Angola material was recalled from the Zoological Museum Hamburg and by re-examination confirmed as fitting with the morphology of the specimen from the Cape Verdes. All other so far published records of *P. calloplura* came from more northern, less deep sublittoral to bathyal waters of the NE-Atlantic (and off Japan). The previously published data did not suffice to evaluate whether there are latitudinal clines rather than a clear-cut separation of morphological clusters. In order to shed light on this question, requests for loan of northern material were sent to museums and respective experts. The Hamburg Museum provided a single, somewhat damaged, specimen (not labeled as type) sampled by E.W.L. Holt, first author of the first description of *P. calloplura*, in the Celtic Sea near the range estimated by Wittmann (2020) for the originally undefined type locality. Inmaculada Frutos from the University of Łódź kindly provided 15 specimens sampled in the frame of the ECOMARG 2004 project in the Bay of Biscay (I. Frutos, pers. communication). Particularly, the examination of dissected materials revealed clear-cut morphological differences between northern and southern specimens, the latter described as a new species of *Parapseudomma* herein.

MATERIALS AND METHODS

Materials were obtained on request from the Zoological Museum Hamburg, from the Naturalis Biodiversity Center in Leiden, and from Inmaculada Frutos, University of Łódź. Materials, including the here defined types, were returned in vials with aqueous solution of ethanol 80% with propylene glycol 10% unless explicitly stated as having been dissected and mounted on slides.

Terminology, measurements, preparation, microscopy, and documentation as in Wittmann and Chevaldonné (2021). Nomenclature from genus to family level according to Wittmann et al. (2014). All here studied eye rudiments are proximally united in a transverse bar rather than a plate, therefore termed ‘eye-bars’ rather than using the traditional term ‘eyeplates’. Unlike ‘claws’, the ‘nails’ are not hook-like; only nails were found in the here treated species. Wittmann and Chevaldonné (2021) described a pit-like depression with striated pad on the bottom, probably a sensorial structure, dorsally on the basal segment of the antennula. This organ is here termed ‘antennular bursa’ (Fig. 4E). Wittmann and Chevaldonné (2021) also described an ‘eyeplate cyst’, for conformity now termed ‘eye-cyst’ (Fig. 2C) found inside fused eye-bar; this cyst opens to the outside or into the eye cleft by a duct.

Abbreviations

= station number of the DIVA-1 expedition
 BL = body length measured from tip of rostrum to terminal margin of telson
 DD = decimal degrees of geographic coordinates
 RMNH = Rijksmuseum van Natuurlijke Historie, Naturalis Biodiversity Center in Leiden
 ZMH = Zoological Museum Hamburg, also named Museum of Nature Hamburg
 e.n. = epinet of epibenthic sledge
 n.n. = net of epibenthic sledge not specified
 s.n. = supranet of epibenthic sledge

SYSTEMATICS

Family Mysidae Haworth, 1825

Subfamily Erythropinae Hansen, 1910

Diagnosis of this subfamily as in Wittmann et al. (2014). Worldwide key to its currently acknowledged 57 genera plus three new ones will be provided in a forthcoming report about Mysidae of three ANDEEP expeditions to the Antarctic deep sea.

Genus *Parapseudomma* Nouvel and Lagardère, 1976

Pseudomma — Lo Bianco, 1903: 273 (records, Gulf of Naples). — Holt and Tattersall, 1905: 126 (in part, NE-Atlantic records). — Tattersall, 1909: 136 (in part, key to species). — Zimmer, 1909: 99, 100 (in part, definition, key to species). — Tattersall and Tattersall, 1951: 232 (in part, key to NE-Atlantic species).

Parapseudomma Nouvel and Lagardère, 1976: 1311–1317, figs. 206–225 (diagnosis, description). — Meland and Willassen, 2004: fig. 4 (molecular phylogeny). — Fukuoka and Murano, 2006: tab. III (modification of pleopods). — Wittmann et al., 2014: 247, 337 (morphology, taxonomy). — San Vicente, 2017: tab. 2 (biogeography). — Mees and Meland, 2022: AphiaID 119893 (accepted).

Species inventory and distribution.

- *Parapseudomma calloplura* (Holt and Tattersall, 1905), NE-Atlantic, Mediterranean, off Japan, depth 94–1200 m.

- *Parapseudomma stenurum* n. sp., E-Atlantic: off Cape Verde Islands, Angola Basin, depth 3825–5460 m.

Type species. *Pseudomma calloplura* Holt and Tattersall, 1905, by monotypy.

Revised diagnosis. The diagnosis by Nouvel and Lagardère (1976) is revised to include *P. stenurum* n. sp. and recently detected sensorial organs. Carapace with widely rounded anterior margin. Eye rudiments together forming transverse, dorsoventrally flattened bar proximally fused and distally separated by narrow, median cleft proximally leading to eye-cyst (Fig. 2A, C); no visual elements, no eye papilla. Antennula with antennular bursa (Fig. 4E); largest lobe (Fig. 5A) of trunk arising dorsally near disto-mesial edge of basal segment (unlike disto-laterally as in most mysids). Antennal peduncle three-segmented. Antennal scale with 0–1 small apical segment; its mesial margin setose and its bare, straight lateral margin ending in tooth. Labrum mid-anteriorly slightly prolonged.

Mandibles with major components well developed except for right digitus mobilis smaller (Fig. 1C) than left digitus or even reduced to spine (Fig. 4B). Posterior thoracomeres of non-adults with median sternal process, no such processes in adults. Thoracic endopods 3–8 with 2–3-segmented carpopropodus. Marsupium formed by 3 pairs of oostegites. Endopod of uropods with 0–1 small spine near statocyst. Telson trapezoid with convex terminal margin; lateral margins with smooth spines, terminal margin with hispid spines (Fig. 4D), no setae.

Potential additional diagnostic characters. Adult male pleopods in type species with large sympod, endopods 2–5 and all exopods multisegmented; pleopod 4 the largest, penultimate segment of its endopod with large, modified seta. Adult males unknown in *P. stenurum* n. sp.

***Parapseudomma calloplura* (Holt and Tattersall, 1905)**
(Figs. 1, 2)

Pseudomma affine — Lo Bianco, 1903: 245, 253, 276 (records, Gulf of Naples).

Pseudomma calloplura Holt and Tattersall, 1905: 126 (preliminary diagnosis). — Holt and Tattersall, 1906: 30–32, figs. 1–5 in pl. IV (description, NE-Atlantic records). — Tattersall, 1909: 133, tab. 3, figs. 7–12 in pl. 7 (description, Mediterranean records). — Zimmer, 1909: 106, figs. 211–213 (description, distribution). — Băcescu, 1941: 19–21, fig. 7 (description, W-Mediterranean record). — Tattersall and Tattersall, 1951: 236–238, fig. 53A–G (NE-Atlantic, description, taxonomy). — Murano, 1970: 142, figs. 10–13 (first Pacific records).

Parapseudomma calloplura — Nouvel and Lagardère, 1976: 1311–1317, figs. 206–225 (description, revised generic assignment). — Mauchline, 1986: 814 (biology, NE-Atlantic records). — Băcescu, 1989: 119 (record from Alboran Sea). — Cunha et al., 1997: 128, tabs. 5, 9 (Iberian seas, depth range). — Cartes and Sorbe, 1998: 283–285, figs. 5, 7 in

tab. VII (feeding). — Cartes et al., 2001: 2226, tabs. 1–5, fig. 3 (life history, secondary production). — Meland and Willassen, 2007: tab. 2, fig. 3 (phylogeny, rRNA sequencing). — Petryashov, 2009: tab. 1 (biogeographic analysis). — Wittmann et al., 2014: 337, fig. 54.21 (morphology, taxonomy). — San Vicente, 2017: tab 3, fig. 4 (distribution, Iberian Peninsula). — Astthorsson and Brattegard, 2022: 65, fig. 75 (distribution, Iceland). — Mees and Meland, 2022: AphiaID 120165 (accepted). — Ríos et al., 2022: tab. 1 (submarine canyons, Cantabrian Sea).

Material examined. 1 adult male in 2 parts, originally labeled as *Pseudomma calloplura* (BL about 8 mm), ZMHK 11194, Celtic Sea, slope from Celtic shelf down to Porcupine Seabight, 144 km SW of Ireland, DD 50.35 -011.00, 625–631 m depth, L.R. 448, coll. E.W.L. Holt Dept. Agricult. Fish. Br. — 5 subadult males (BL 6.1–7.5 mm), 2 subadult females (BL 5.6–6.3 mm), 3 immature females (BL 4.8–5.7 mm), 1 immature male (BL 5.0 mm), 3 juveniles (BL 3.1–4.0 mm) in vial plus 1 subadult male (BL 7.8 mm) on slides, Bay of Biscay, Le Danois Bank, DD 42.67 -011.74, 500–496 m depth, ECOMARG 2004 with R/V “Vizconde de Eza”, E04-TS5, 12–30 April 2004, coll. Inmaculada Frutos.

Distribution. Type locality not stated by Holt and Tattersall (1905). A rough estimate by Wittmann (2020) suggests that the type locality is off Ireland in the range of 52–54°N 12–13°W, depth 363–696 m. The present sample from the Celtic Sea was taken near this range by E.W.L. Holt, the first author of the first description. This species is known from the NE-Atlantic and Mediterranean, 35–58°N 013°W–014°E, depth 94–1200 m (references listed above); the here presented records are within these ranges. Murano (1970) reported this species as *Pseudomma calloplura* from the NW-Pacific off Japan, 35–37°N 137–140°E, depth 220–660 m. Records of *Parapseudomma calloplura* reported by Wittmann (2020) from the Angola Basin are here attributed to the below described *Parapseudomma stenurum* n. sp.

Revised diagnosis. Based on adults of both sexes. All features within the limits of the genus diagnosis. Carapace without rostrum; disto-lateral edges angular (right-angled to wide-angled). Transverse extension of eye-bar 2.3–3.5 times length of distal segment of antennular trunk. Eyes fused at proximal third, while distally separated by narrow median cleft (Fig. 2A). Eyes dorsoventrally flattened by factor of 1.4–2.2 measured at maximum width in dorsal view. Each eye microserrated (Fig. 2B) along central third to half of its anterior margin. Disto-mesial lobe dorsally at basal segment of antennular trunk reaching to half-length of median segment. Disto-lateral edge of antennal sympod with tooth-like projection. Antennal scale with small apical segment separated by tiny (in part inconspicuous) suture. Length of scale 3.5–5.0 times maximum width; mesial margin setose; straight lateral margin bare, ending in tooth; distal segment not reaching to tip of this tooth. Scale extending 40–55% its length beyond antennal peduncle and 35–50% beyond antennular trunk. Labrum mid-rostrally slightly prolonged by small acute projection. Mandibles normal, right digitus mobilis smaller than the left one (Fig. 1C). Unsegmented carpus of thoracic endopods 3–8 separated from two-segmented propodus by oblique articulation. Male pleopod 4 the largest, penultimate segment of its endopod with large smooth (modified) seta in adults longer than endopod. Exopod of uropods extending beyond endopod; exopod and endopod beyond telson (Fig. 1A, B). Endopod with 1 small spine on mesial margin below statocyst. Telson (Fig. 2E) with slightly sigmoid, almost straight lateral margins and convex, broadly rounded terminal margin. Telson length 1.7–2.9 times maximum width near basis and 4–6 times width at disto-lateral edge. Proximal 29–45% of lateral margins smooth, remaining distal portion of each margin with 10–15 spines distally somewhat discontinuously increasing in size. Terminal margin with minute (often inconspicuous) median spine flanked by 3–4 pairs of large spines; these spines bilaterally armed along their basal to subapical portions with stiff bristles; largest spine 23–34% telson length.

Supplementary notes. Based on adult male and subadults of both sexes. Acute median process from clypeus anteriorly extending shortly beyond eye-bar. Flagellum of thoracic exopod 1 nine-segmented, flagella 2–8 ten-segmented. Thoracic endopods 1–7 increasing in length and slenderness caudally (endopod 8 not available); endopods 3–7 reach at least to mid of antennular trunk when stretched anteriorly. Endopods 1, 2 with short but strong, weakly curved, smooth nail; nail 1 thrice length of dactylus 1, nail 2 twice length of larger dactylus 2. Endopods 3–7 with slender, needle-like, slightly curved nail increasing in length caudally together with its respective endopod. Juveniles with pair of paramedian sternal processes on thoracomere 2, and single mid-sternal process on each thoracomere 3–8. There are on average fewer such processes (Fig. 2D) in immatures of both sexes, versus none in adult male. Statoliths composed of fluorite, diameter 0.15–0.26 mm ($n = 4$ statoliths from two subadults).

Male sexual characteristics. Size and structure of thoracic exopods are non-dimorphic when comparing equally sized subadults (adult females not available). Exopod of adult and subadult male pleopods 2–4 with short spine-like seta (besides other setae) at penultimate segment; pleopod 5 with group of three small, supernumerary setae in the respective position.

Adult male with BL 8 mm from the Celtic Sea with large, strongly setose appendix masculina about as long as terminal segment of antennular trunk; appendix extending by 3/4 its length beyond this segment. Thoracomeres 2–8 without mid-sternal processes, not counting usual rostral lobe from sternite 1 contributing to caudal closure of mouth area. Penes slightly longer than basal plate of thoracic exopod 8. Spermatozoa visible in efferent ducts. Endopod of pleopods 1–5 with 1, 13, 13, 13, 13 segments, exopod with 12, 14, 13, 13, 13 segments, respectively. Male-specific smooth seta with 1.6 times endopod length arising from penultimate segment of endopod of pleopod 4.

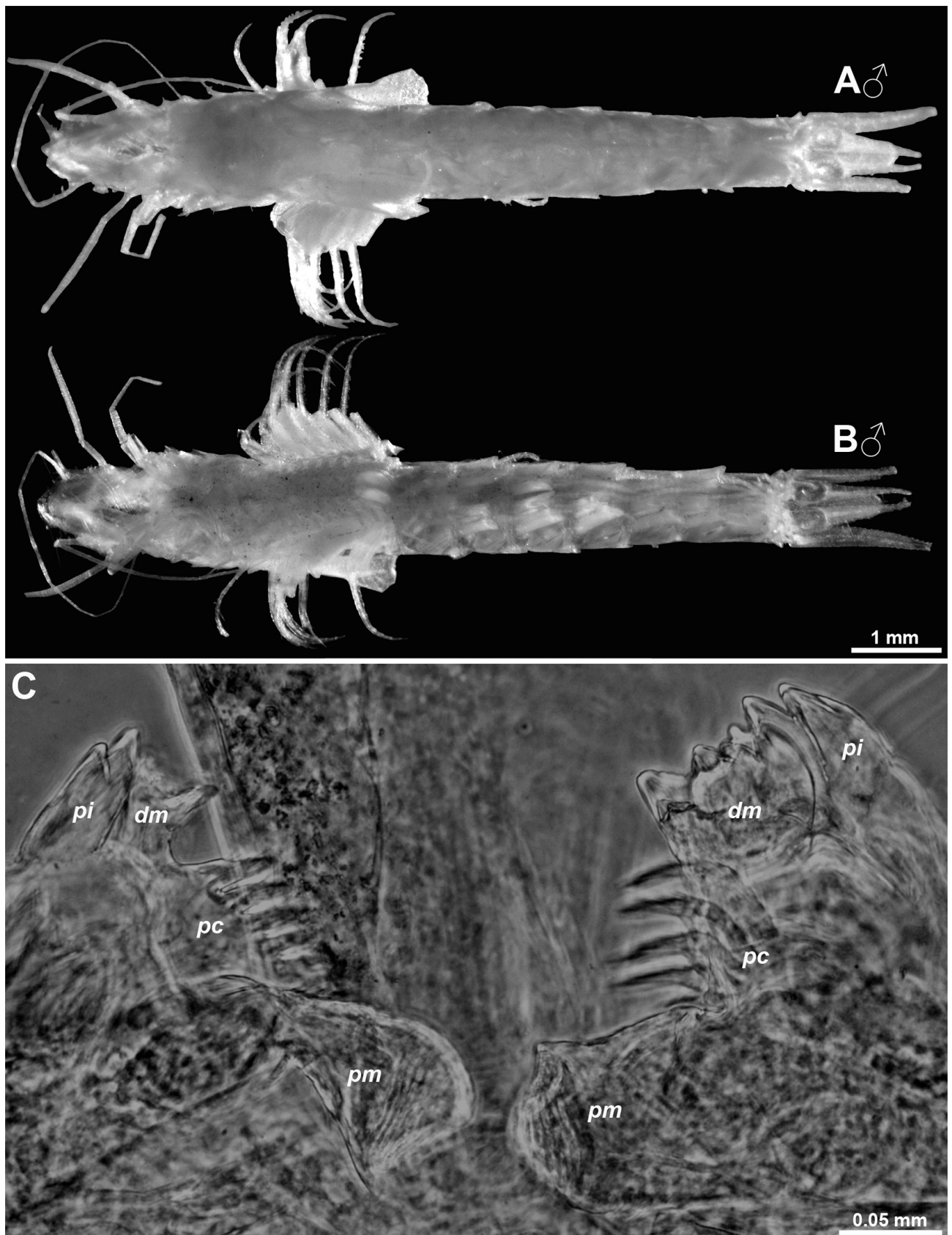


Figure 1. *Parapseudomma calloplura* (Holt and Tattersall, 1905), subadult males with BL 7.8 mm (**A, B**) and 7.5 mm (**C**) from the Bay of Biscay. **A, B**, Subadult in toto, dorsal (**A**) and ventral (**B**); **C**, masticatory portion of right (to the left) and left (to the right) mandible with pars incisiva (pi), digitus mobilis (dm), spines of the pars centralis (pc) and pars molaris (pm), caudal. **A, B**, object artificially separated from background.

The largest available subadult male with BL 7.8 mm from the Bay of Biscay (Fig. 1A, B) with same-sized though less setose appendix masculina and with about same-sized penes (Fig. 2D) compared with the adult from the Celtic Sea. Spermatozoa visible in efferent ducts despite certain subadult characters in this specimen, namely thoracic sternum 8 (Fig. 2D) with well-developed, hispid, distally blunt, mid-sternal process, sternum 7 with vestigial non-hispid process, while sterna 2–6 without such processes. Endopod of pleopods 1–5 with 1, 13, 12–13, 13, 11 segments, exopod with 11, 14, 12–13, 13, 12 segments,

respectively; penultimate segment of endopod of pleopod 4 with male-specific seta shorter than small ultimate segment. The respective seta 0.4 times endopod length in a subadult male with BL 7.5 mm. Pleopod 4 of the latter specimen with 12-segmented endopod and 13-segmented exopod. Pleopod 4 with 8-segmented endopod and 8-segmented exopod in subadult with BL 7.3 mm. All pleopods uniramous and unsegmented in immature male with BL 5.0 mm; its penes one third length of basal plate of thoracic exopod 8, no spermatozoa visible; appendix masculina vestigial.

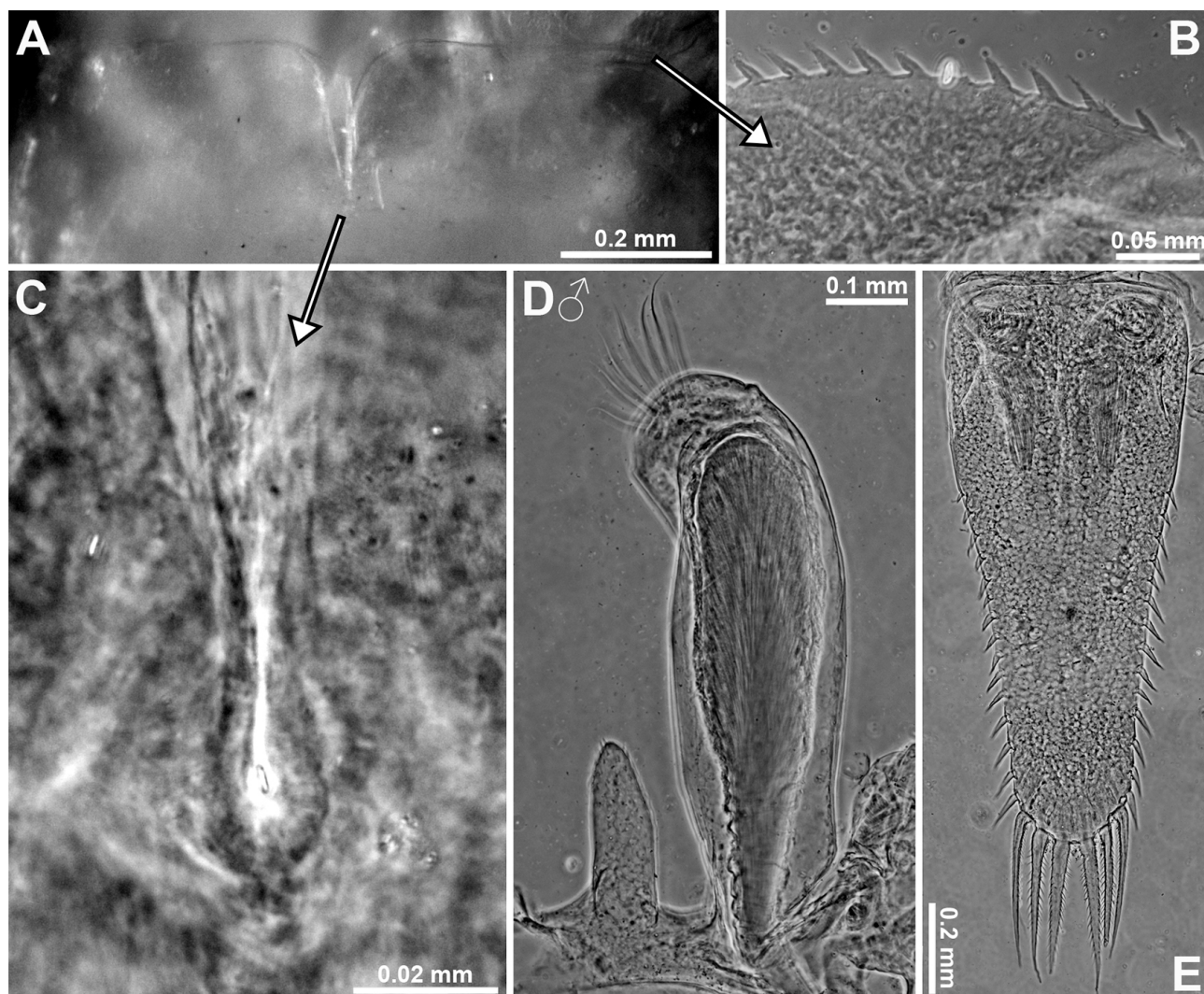


Figure 2. *Parapseudomma calloplura* (Holt and Tattersall, 1905), subadult male with BL 7.8 mm from the Bay of Biscay. **A**, Eye rudiments, dorsal; **B**, detail of panel (A) showing serrated portion of anterior margin of right eye rudiment; **C**, detail of panel (A) showing median eye-cyst; **D**, thoracic sternite 8 with median process and penis; **E**, telson.

***Parapseudomma stenurum* n. sp.**

(Figs. 3–6)

<https://zoobank.org/urn:lsid:zoobank.org:act:4FC1ECE8-5E91-4246-B078-311A9E9F91CE>

Parapseudomma calloplura — Wittmann, 2020: 18, 19, tab. 1.

Type material. Holotype: adult female (BL 24.9 mm) completely dissected, on 12 slides numbered in series of RMNH.CRUS.21840 to RMNH.CRUS.21851, Cape Verde Islands, S of Santiago, DD 14.517–023.55, 3825–4025 m depth, deep-sea clay, 3.5 m Agassiz trawl, expedition CANCAP-VI, sta. 6.018, 5 June 1982. — Paratypes: 1 adult female (BL 20.0 mm), 1 juvenile, fragments of 1 immature, ZMH 58263, Angola Basin, start DD 22.3323 003.3057, end DD 22.3375 003.3073, 5179–5179 m depth, n.n., #318, 9 July 2000. — 1 adult female (BL about 23.3 mm), head broken, ZMH 58264, Angola Basin, start DD 22.3319 003.2993, end DD 22.3342 003.2993, 5161–5162 m depth, n.n., #320, 10 July 2000. — 2 damaged immatures (BL ca. 6.1, 7.0 mm), ZMH 58266, plus separate vial with 1 immature female (BL 9.4 mm), ZMH 58265, Angola Basin, start DD 17.0823 004.6801, end DD 17.1242 004.7046, 5460–5460 m depth, n.n., #344, 25 July 2000. — 1 subadult female (BL 21.1 mm) plus 1 subadult female (BL about 14 mm) with tailfan missing, ZMH 58267, same sample as before, s.n. — 1 subadult female (BL 17.2 mm), ZMH 58268, same sample as before, e.n. — 1 immature male (BL 11.2 mm), ZMH 58269, Angola Basin, start DD 16.2222 005.4473, end DD 16.2470 005.4450, 5433–5434 m depth, e.n., #350, 29 July 2000.

Diagnosis. Based on adult females. All female features within the limits of the genus diagnosis. Carapace with rounded disto-lateral edges; rostrum short and broadly rounded (Fig. 4F), slightly uptilted (Fig. 3C). Eye rudiments fused at proximal half (of antero-posterior extension), distally separated by narrow median cleft (Fig. 3D). Transverse extension of eye-bar 1.8–2.5 times length of distal segment of antennular trunk. Eye rudiments dorsoventrally flattened by factor of 1.6–1.8 measured at maximum antero-posterior extension in dorsal view; anterior

margin not serrated. Disto-mesial lobe dorsally at basal segment of antennular trunk reaching to distal margin of median segment. Disto-lateral edge of antennal sympod angular, no tooth-like projection. Antennal scale not subdivided, no apical lobe (Fig. 5C). Length of scale 3.4–3.6 times maximum width. Scale extends 50–60% its length beyond antennal peduncle and 50–70% beyond antennular trunk. Labrum mid-anteriorly slightly produced, tip rounded (Fig. 5E). Mandibles with pars incisiva, pars centralis and pars molaris well developed; right digitus mobilis reduced to slender spine (Fig. 4B), left digitus essentially normal, though more slender than in most mysids (Fig. 4A). Carpopropodus of thoracic endopods 3–8 with 2–3 segments separated by transverse articulations. Endopod of uropods without spine (Fig. 3F). Telson (Figs. 3F, 4D, 6K) elongate trapezoid, slender, with slightly sigmoid, almost straight lateral margins. Telson length 2.7–3.0 times maximum width near basis and 10–14 times width at disto-lateral edge; narrow terminal margin convex. Proximal 23–25% of lateral margins smooth, remaining distal portion of each margin with 17–23 spines distally somewhat discontinuously increasing in size; terminal margin with 3–4 pairs of large spines. Terminal spines bilaterally lined by minute stiff bristles along basal 50–70% of their margins (Fig. 4D); largest spine one seventh telson length; no unpaired median spine.

Description of the holotype. All female features within the limits of the species diagnosis. Female with 24.9 mm body length, marsupium empty (Fig. 3A). Rostrum contributing 0.6% to body length, carapace 23% (without rostrum), thorax 32%, pleon 49%, and (long) telson 19%. Parts of body cuticle ornamented with fields of minute, roughly ellipsoidal shallow depressions (Fig. 4C), some of which (accidentally) filled with external material. Tergites of thoracomere 8 and of adjoining pleomeres 1, 2 almost completely ornamented, carapace mainly on fields illustrated as shaded areas in Fig. 5D. Minor numbers of such depressions present on antennular trunk and antennal peduncle, again fewer on basal plates of thoracic exopods. Minute ‘cils’ (4–7 µm long slender scales) line outer margin and parts of dorsal face of eye rudiments.

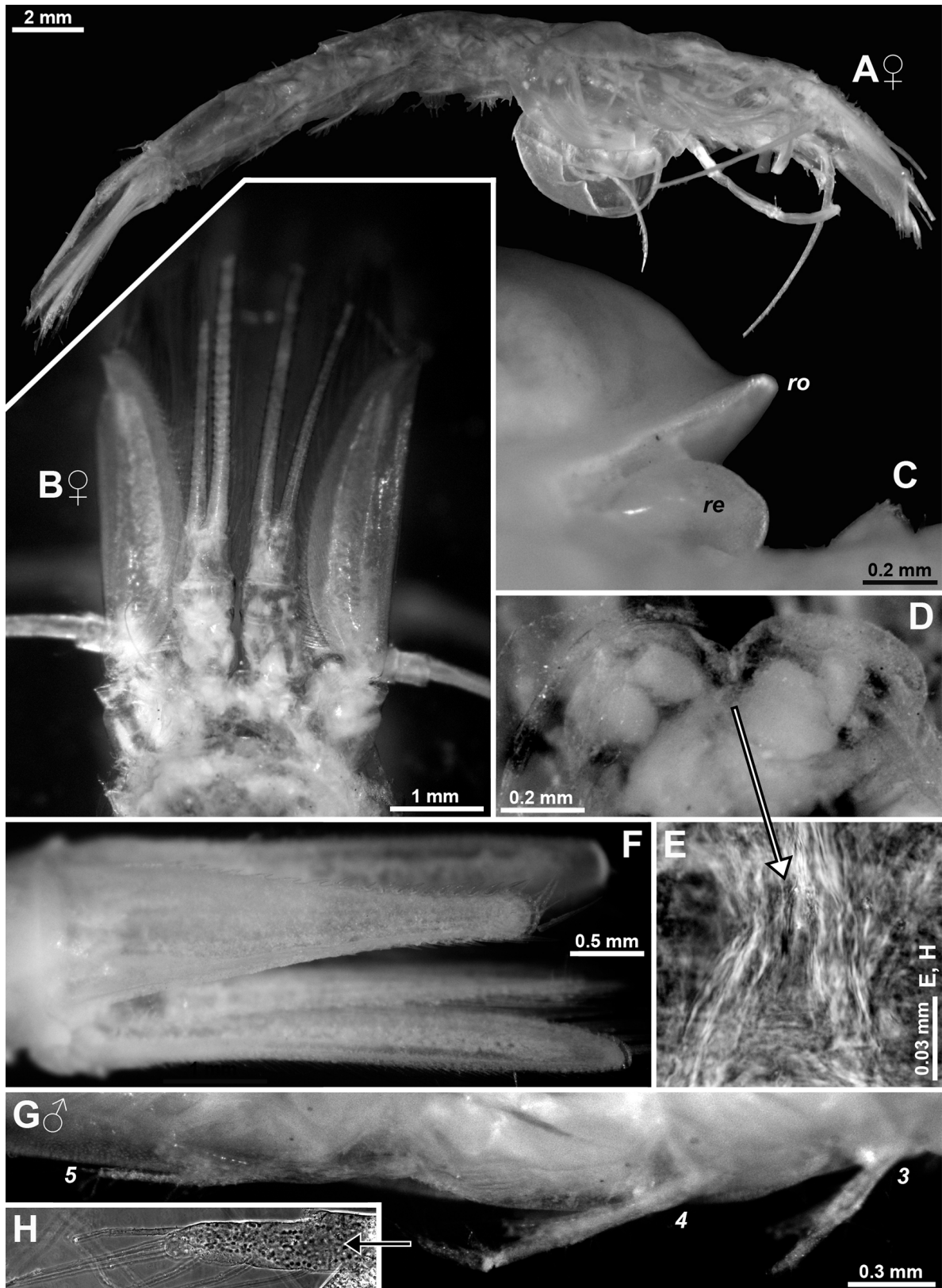


Figure 3. *Parapseudomma stenurum* n. sp., holotype adult female with BL 24.9 mm (**A**, **B**, **E**) from the deep sea off Cape Verde Islands, and paratypes subadult female 14 mm (**C**), immature male 11.2 mm (**D**, **G**, **H**) and adult female 17.1 mm (**F**) from the Angola Basin. **A**, Female holotype in toto, lateral (most thoracic endopods broken); **B**, cephalic region of holotype, dorsal; **C**, rostrum (ro) and right eye rudiment (re), lateral; **D**, eye rudiments, dorsal; **E**, detail of panel (**D**) showing median eye-cyst in a larger specimen (holotype), dorsal. **F**, tail fan, dorsal; **G**, pleopods 3–5 in loco, lateral; **H**, detail of panel (**G**) showing tip of pleopod 4. **A**, two photos mounted together; **A**, **C**, objects artificially separated from background.

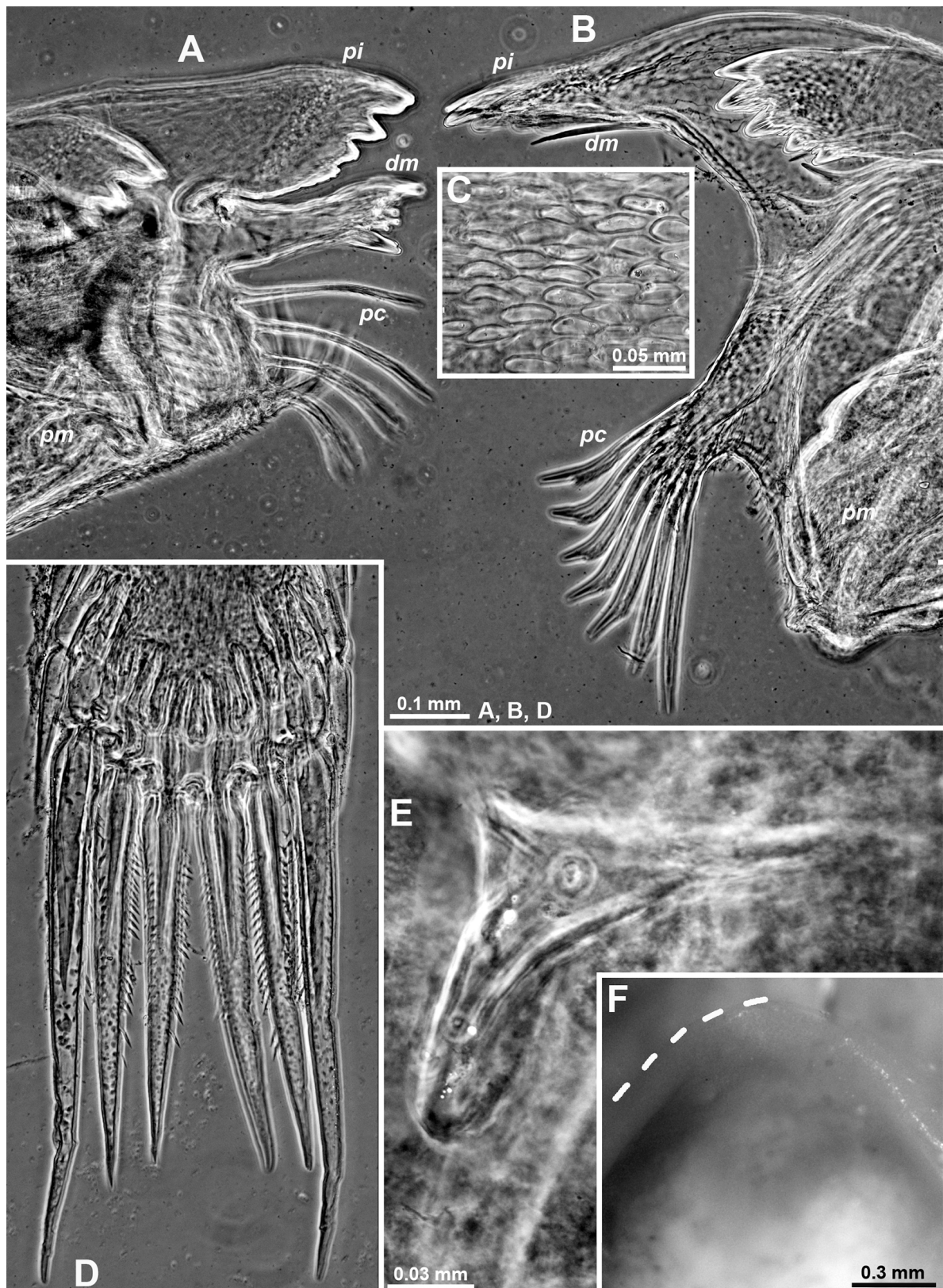


Figure 4. *Parapseudomma stenurum* n. sp., holotype adult female with BL 24.9 mm (A–E) from the deep sea off Cape Verde Islands and paratype subadult female 14 mm (F) from the Angola Basin. **A, B**, Masticatory portions of left (A) and right (B) mandibles with pars incisiva (pi), digitus mobilis (dm), spines of the pars centralis (pc) and pars molaris (pm), rostral; **C**, cuticular ornamentation on parts of the carapace indicated by shaded fields in Fig. 5D; **D**, distal portion of telson, dorsal; **E**, antennular bursa, dorsal; **F**, rostrum with respective portion of carapace, dorsal, dashed line enhances the left anterior margin of the rostrum. **A, B, D**, structures of the subsequent molt stage visible inside objects.

Carapace (Fig. 5D) with disto-lateral edges well rounded. Cervical sulcus distinct, no cardinal sulcus visible. Posterior margin weakly concave. Carapace leaving 1.5 thoracic segments mid-dorsally exposed (as in other mysids the coverage may vary with swelling of the thorax due to yolk accumulation in the ovarian tubes).

Antennula (Figs. 3B, 5A, B). Transverse articulations between three segments of trunk. Segments 1–3 contributing 49%, 22%, and 29% to total trunk length, respectively. Setose lobe dorsally in about median position shortly behind anterior margin in each segment. Median lobe of distal segment with 3 barbed setae and transverse series of 3 teeth (Fig. 5B). Tooth size increasing laterally. Basal portion of outer flagellum 0.8–0.9 times as wide as in inner flagellum.

Antenna (Figs. 3B, 5C). Sympod two-segmented, caudally in addition with end sac of antennal gland. Peduncle with 3 segments separated by transverse articulations. Basal segment contributing 30%, median segment 43%, and terminal segment 27% to total length. Basal segment smooth, median and terminal segments each with few barbed setae.

Labrum as in diagnosis and in Fig. 5E, damaged labium as in Fig. 5G, mounting of foregut failed.

Mandibles (Figs. 4A, B, 5F). Palp three-segmented with basal segment contributing 12–13%, median segment 62–63%, and terminal segment 24–26% to total palp length. Palp not hispid, its basal segment without setae, median segment with sparse setation on both lateral margins. Length of median segment 4 times maximum width, lateral margin slightly sigmoid while mesial margin sigmoid with near-median convex portion more strongly curved than proximal concave portion. Terminal segment 2.3–2.9 times as long as broad and 0.4 times as long as median segment. Terminal segment well setose, with longitudinal series of setae on distal 3/4 of rostral face. Right mandible (Fig. 4B) with 5 large teeth on pars incisiva; digitus mobilis reduced to slender, subapically slightly microserrated spine; pars centralis with large spine-free portion proximally followed by large lobe apically bearing seven long spines; these spines microserrated by acute bristles along their subbasal to subapical portions. Processus molaris of each mandible with strongly cuticularized masticatory lamellae. Left mandible (Figs. 4A, 5F) normal, its pars incisiva with

4 large teeth; digitus mobilis with long, slender basis and with 2 large, plus more than 4 small teeth on apex; pars centralis all along with 12 slender spines bearing stiff bristles (only 4 spines roughly in focus in Fig. 4A, all 12 spines visualized in Fig. 5F).

Maxillula (Fig. 5H). Distal segment with 15 strong, bluntly serrated spines on transverse terminal margin. This segment subterminally with transverse series of 9 setae bearing long stiff barbs. Basal segment furnished with mainly longitudinal though basally bent, comparatively long series of densely set long hairs. Endite terminally with 3 large, distally spiny (by stiff bristles) setae flanked by shorter barbed setae. Two most proximal setae of endite much longer and more slender compared with their distally neighboring setae.

Maxilla (Fig. 5I) densely setose, without spines. Sympod with 3 mesial, only distally strongly setose lobes. Exopod extending to distal margin of basal segment of palp. Exopod with numerous plumose setae all along lateral margin; longest seta at tip, mesial margin with only 3 much shorter plumose setae in subapical position. Palp two-segmented, apical segment 1.1 times as long as basal segment. Apical segment 1.8 times longer than maximum width. Its transverse terminal margin densely setose, lateral margin sparsely setose, mesial margin with only 2 setae near disto-mesial edge. Basal segment basally broader, on rostral face (below drawing plane in Fig. 5I) near mesial margin with longitudinal series of 7 densely barbed, basally thick setae (visualized by dashed lines).

Thorax (Fig. 6A–H). Sternite 1 with distally rounded mid-rostral lobe. Sternites 2–8 without mid-ventral processes. Basal plates of exopods 1, 8 with length twice maximum width; plates 2–7 with twice maximum width. Disto-lateral edge with small tooth-like projection in all basal plates. Flagellum of exopod 1 with 8 segments, flagella 2–8 with 9 segments. Endopods 1, 2 with 6 segments, endopods 3–8 broken.

Sympod of thoracopod 1 (Fig. 6A) with small mesial lobe bearing 1 plumose seta at tip. Basis of endopod 1 with very large setose endite, remaining segments without endite. Endopod 1 densely setose along mesial margin, less along lateral margin; its smooth apical nail (Fig. 6B) 1.6 times as long as dactylus. Epipod 1 (Fig. 6A) linguiform with narrowly blunt apex, length 0.9 times that of basal plate of exopod 1. Epipod subapically with 3 minute setae.

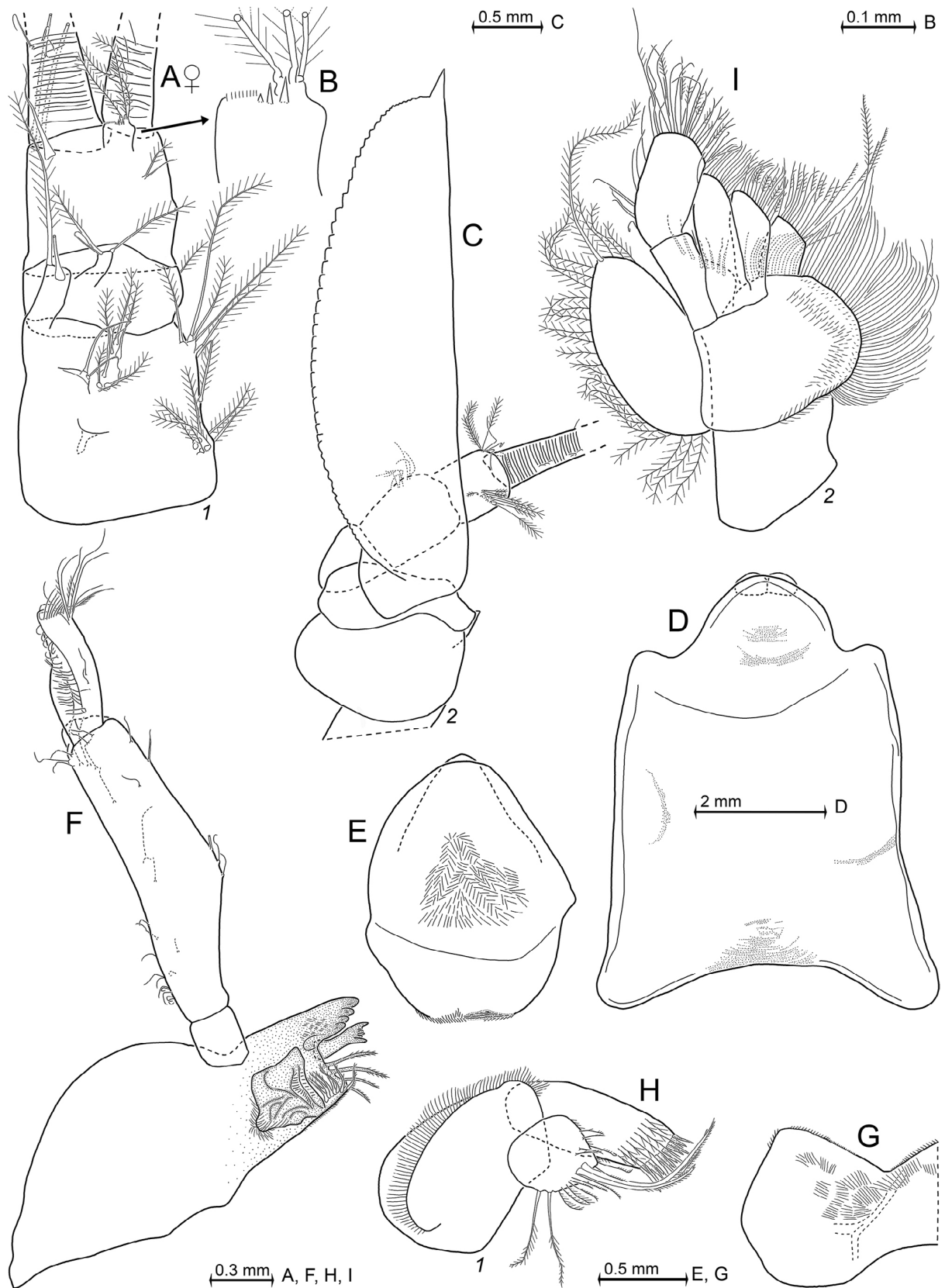


Figure 5. *Parapseudomma stenurum* n. sp., holotype adult female with BL 24.9 mm from the deep sea off Cape Verde Islands. **A**, Right antennula, dorsal; **B**, detail of panel (**A**) showing lobe about mid-dorsally at distal segment of antennular trunk; **C**, right antenna, dorsal; **D**, carapace with eye rudiments expanded on slide, dorsal, shaded fields indicate cuticular ornamentation as in Fig. 4C; **E**, labrum, dorsal (= oral) face; **F**, left mandible with palp, rostral; **G**, labium, caudal, left lobe (visualized to the right) damaged; **H**, maxillula, caudal; **I**, maxilla, caudal.

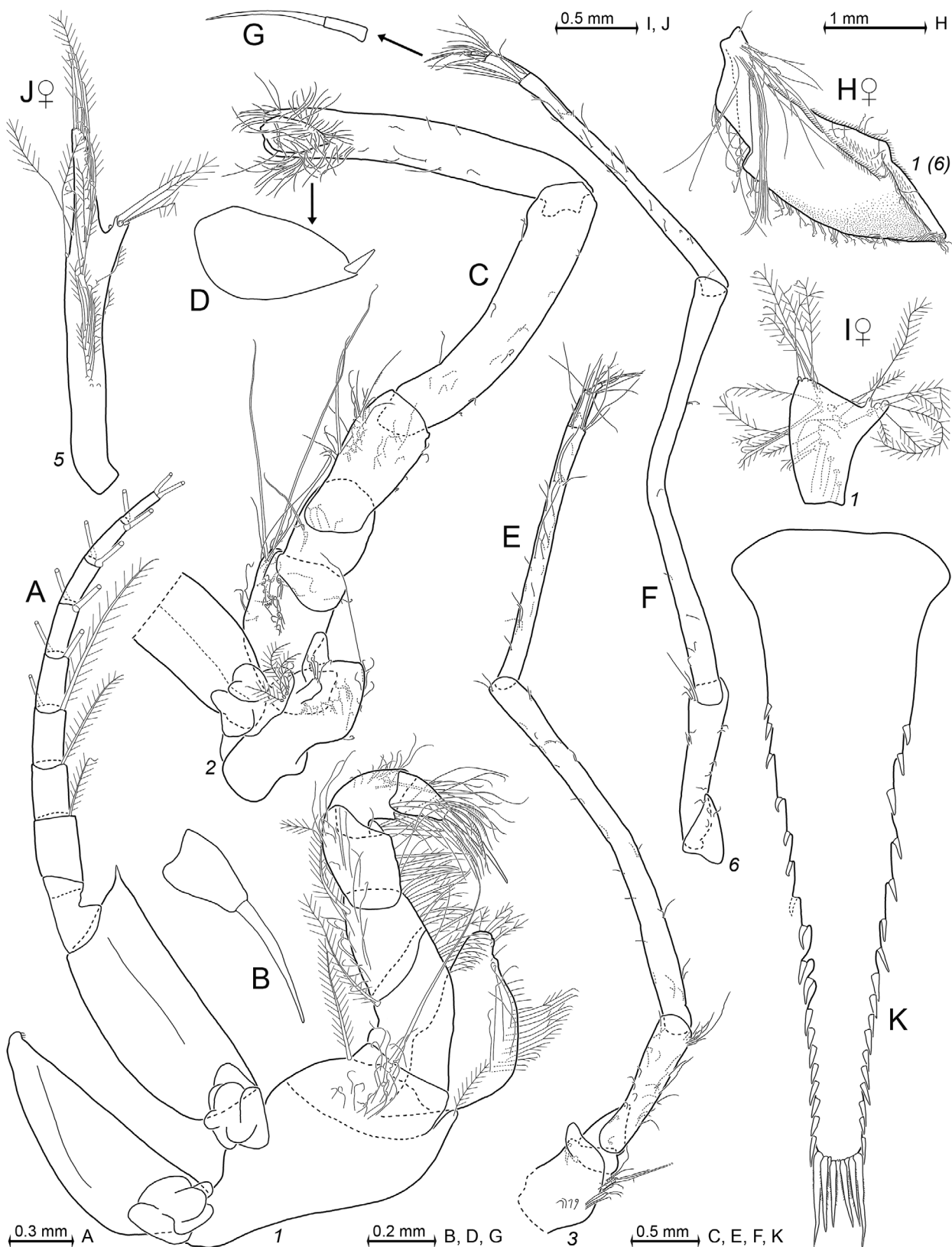


Figure 6. *Parapseudomma stenurum* n. sp., holotype adult female with BL 24.9 mm (**A–D**, **H–K**) from the deep sea off Cape Verde Islands and paratype subadult female 14 mm (**E–G**) from the Angola Basin. **A**, Thoracopod 1 with epipod, caudal; **B**, detail of panel (**A**) showing dactylus 1 with nail, setae omitted; **C**, thoracic endopod 2 with sympod and part of exopod, rostral; **D**, detail of panel (**C**) showing dactylus 2 with nail, setae omitted; **E**, thoracic endopod 3 with sympod; **F**, thoracic endopod 6 without basis (sympod); **G**, detail of panel (**F**) showing dactylus 6 with nail, setae omitted; **H**, oostegite 1, inner (= mesial) face, shaded fields stand for areas with minute acute scales; **I**, pleopod 1, caudal (= mesial) face; **J**, pleopod 5, rostral (= lateral) face; **K**, telson.

Endopod 2 (Fig. 6C, D) without endites. Two very long setae reaching from disto-mesial edge of basis beyond ischium. Dactylus reflexed, densely setose, remaining segments less setose. Dactylus with short thick nail (Fig. 6D) hidden in the dense jungle of setae.

Marsupium (Figs. 3A, 6H). Proximal portion of oostegite 1 with dense brush of setae on inner face (inside marsupium). These comparatively long setae microserrated by series of stiff, acute bristles along their distal half. Less dense brush of such setae on oostegite 2, again less dense on oostegite 3. Oostegite 1 with small smooth setae along most of ventral margin and on distal half of dorsal margin, the latter margin partly folded inward (artificially) in Fig. 6H. Coverage by tiny hairs on and near dorsal margin. Shaded fields in Fig. 6H visualize areas with minute acute scales. Most of dorsal margin smooth in oostegites 2, 3. These oostegites with ventral and anterior margins plus part of posterior margin bearing barbed setae contributing to ventral and caudal, ventilation-pervious closure of marsupium. Only oostegites 2, 3 with smooth, slender whip setae loosely scattered over most of outer face; no scales on both faces.

Pleon including tail fan (Figs. 3A, F–H, 6I–K). Pleonites 1–5 measuring 0.5–0.6 times length of pleonite 6; the value being 1.4 for exopod of uropods, 1.3 for endopod, and 1.2 for telson. Both length and slenderness of pleopods 1–5 increasing caudally, setation as in Fig. 6I, J. Scutellum paracaudale subtriangular, distally continuously rounded. Exopod of uropods extending 0.1 times its length beyond endopod and 0.2 beyond telson; endopod 0.1 times its length beyond telson (Fig. 3F). Statoliths composed of fluorite, diameter 0.18–0.19 mm. Telson with total of 41 spines, comprising 17 plus 18 small smooth spines on lateral margins along with 2 × 3 large, hispid spines on terminal margin.

Supplementary data from paratypes. All paratypes stem from the deep sea of the Angola Basin. Immature male with BL 11.2 mm showing right mandible as in holotype (Fig. 4B). Its left mandible also as in the holotype (Fig. 4A) except for two meristic differences, namely digitus mobilis with 2 large plus 3 (versus > 4) small teeth on apex and pars centralis all along with 8 (versus 12) slender spines.

Immature female with BL 9.4 mm showing hispid, anteriorly curved, median processes from thoracic sternites 4–8 (nos. 1–3 not inspected). No such processes in adult females. Immature male with BL 11.2 mm with such processes on sternites 2–8, its penes extending shortly beyond sympod 8, appendix masculina still very small; pleopods 1–5 still uniramous (Fig. 3G) with pseudobranchial lobe larger than in female holotype; pleopods 1–3, 5 unsegmented, increasing in length caudally; pleopod 4 not in series by being the largest (Fig. 3G), distally with incipient segmentation (Fig. 3H). No additional males available.

Thoracic endopods 3–8 of both sexes with 7–8 segments (Fig. 6E) counting from basis to dactylus or 6–7 segments (Fig. 6F) from praeischium to dactylus, respectively. Carpopropodites with 2–3 segments separated by transverse articulations (Fig. 6E, F). Dactyli with slender, weakly bent, smooth nail (Fig. 6G).

Statoliths mineralized with fluorite, diameter 0.13–0.17 mm (n = 4 statoliths of two adult females).

Etymology. The species name is an adjective with Latinized neutral ending formed by amalgamation of the Classic Greek adjective *στενός* (narrow) with the noun *ουρά* (tail) referring to the slender telson.

Type locality. E-Atlantic, Cape Verde Islands, about 42 km south of Santiago Island, DD 14.517 -023.55, on the sea floor in 3825–4025 m depth.

Distribution. E-Atlantic, Cape Verde Islands and Angola Basin, total ranges 14°N to 22°S, 05°E to 24°W, depth 3825–5460 m.

DISCUSSION

Definition of the genus Parapseudomma

The eye rudiment structure of the new species fits with the genus *Parapseudomma* and to a lesser extent also with *Pseudomma*, unlike the other 55 currently acknowledged genera of the Erythropinae, and also the remaining (171 minus 57) Recent genera of the Mysidae. *Parapseudomma* is distinguished from *Pseudomma* by (combinations of) a less deep cleft between the proximally fused eye rudiments,

comparatively large dorsal lobe from the disto-mesial edge of the basal segment of the antennular trunk, short rostral process of the labrum, thoracomeres with sternal processes only in non-adults and large hispid spines but no setae on the terminal margin of the telson. Molecular phylogenetic analysis by Kou et al. (2020) placed *Parapseudomma* and *Pseudomma* in different clusters.

The present finding of an eye-cyst (Figs. 2C, 3E) connected by a duct with the bottom of the median cleft distally separating the incompletely fused eye rudiments both in *Parapseudomma calloplura* as well as *P. stenurum* n. sp. coincides with the evidence of such a cyst in *Pseudomma kryotrogloidyum* Wittmann and Chevaldonné, 2021. These three species also share antennular bursae. Eye-cysts and bursae were probably generally overlooked before 2021 and could be expected for many more species of Erythropinae. Future findings could also lessen the overall morphological distance between *Parapseudomma* and *Pseudomma*.

Validity and affiliation of Parapseudomma stenurum n. sp.

With the reservation that adult males are unknown, the new species fits with all above-discussed features distinguishing *Parapseudomma* from *Pseudomma* and consequently it is attributed to the genus *Parapseudomma*. There are some important differences from the type species *Parapseudomma calloplura*: the new species differs by an unsegmented antennal scale, the carpus of thoracic endopods 3–8 separated from the propodus by a transverse rather than oblique articulation, and the digitus mobilis of the right mandible reduced to a slender spine (Fig. 4B) rather than bearing a number of well-developed teeth (Fig. 1C). Many additional minor differences are listed in the above diagnoses and descriptions. Regarding the major differences, it appears necessary to check other Erythropinae which also have a strongly reduced or a completely reduced digitus mobilis of the right mandible.

Abyssomysis cornuta Wittmann, 2020, from the abyssal plain in the Gulf of Guinea shows the digitus mobilis of the right mandible reduced to a slender spine in males and completely reduced in females. The digitus of the left mandible shows a long, slender basis and a well-toothed apex in both sexes of *A. cornuta*. Both sexes of the new species show mandibles

(Fig. 4A, B) most similar to the male but not to the female of *A. cornuta*. The latter species differs from the new species among other features also by distantly set eyestalks, no median cleft on the eye-bar, and by a short triangular telson with bare lateral margins.

The only known male (holotype) of *Xenomysis unicornis* Kou, Meland and Li, 2020, from the hadal zone in the Mariana Trench shows a completely reduced right digitus mobilis as in the opposite sex (females) of *A. cornuta*. The monotypic genus *Xenomysis* Kou, Meland and Li, 2020 deserves special interest because according to Kou et al. (2020) its DNA sequences cluster with *P. calloplura*, although with low support. *Xenomysis* differs from *P. stenurum* n. sp. by eye-bar without median cleft, acute rostrum, carpus of thoracic endopods 3–8 separated from the propodus by an oblique articulation, and by acutely triangular, elongate telson. Several morphological features of *X. unicornis* remain unclear — loan of the type was hindered by the current pandemic situation and by legislative restrictions — only an unpublished photo of the right side of the cephalothorax was received (see Acknowledgements), which did not yield contrasting information. In the present interpretation the eponymous vertical alignment of the rostrum together with the cervical region of the carapace ruptured off the thorax as indicated in fig. 6b, c by Kou et al. (2020) and the great height of the cervical region in fig. 1 (op. cit.) together with the exceptionally large distance between labrum and clypeus in figs. 2d, 6a by Kou et al. (2020) might represent artefacts of accidental transient lateral compression of the cephalic region. This may have forced elongation of the cephalon with resulting stress on the cervical region of the carapace, which in response lifted up from the thorax and levered the rostrum vertically. The present author has observed comparable artefacts in the rostrum of a total of seven specimens of *Euchaetomera typica* G.O. Sars, 1883, and of three other species of Erythropinae with normally anteriorly directed rostrum. The unsegmented exopod of pleopod 3 and the incipient segmentation (as also here in Fig. 3H) of the endopod of pleopod 4 visible in fig. 6f by Kou et al. (2020) could indicate an incomplete status of male maturity despite well-developed penes and appendix masculina in the holotype of *X. unicornis*. The distally setose lateral margin of the antennal scale

in fig. 2a is inconsistent with the bare lateral margins in figs. 2b, d, e, 6a, b by Kou et al. (2020).

Clearly, future findings of fully adult males of *P. stenurum* n. sp. and *X. unicornis* would provide eagerly awaited information on the extent to which they solidify or weaken sequential and morphological differences between *Parapseudomma* and *Xenomysis*.

ACKNOWLEDGEMENTS

The author is greatly indebted to Nancy Mercado and Petra Wagner from the Museum of Nature Hamburg and to Bram van der Bijl and Jeroen Goud from the Naturalis Biodiversity Center in Leiden, for managing loans of materials. Sincere thanks to Inmaculada Frutos from the University of Łódź for loan of *Parapseudomma calloplura* from the Bay of Biscay and to Qi Kou from the Department of Marine Organism Taxonomy and Phylogeny, Chinese Academy of Sciences, for sending an unpublished photo of *Xenomysis unicornis*.

REFERENCES

- Astthorsson OS and Brattegard T 2022. Distribution and biology of Lophogastrida and Mysida (Crustacea) in Icelandic waters. *Fjölrít Náttúrufræðistofnunar*, 58: 1–114. <https://doi.org/10.33112/1027-832X.58>. [In Icelandic, with English abstract]
- Băcescu M 1941. Les Mysidacés des eaux méditerranéennes de la France (spécialement de Banyuls) et des eaux de Monaco. *Bulletin de l'Institut Océanographique de Monaco*, 795: 1–46. <https://www.vliz.be/imisdocs/publications/ocrd/272874.pdf>
- Băcescu M 1989. Contributions à l'étude du genre *Erythropros* (Crustacea, Mysidacea) du voisinage du Détroit de Gibraltar. *Travaux du Muséum d'Histoire Naturelle "Grigore Antipa"*, 30: 119–127.
- Cartes JE and Sorbe J-C 1998. Aspects of population structure and feeding ecology of the deep-water mysid *Boreomysis arctica*, a dominant species in western Mediterranean slope assemblages. *Journal of Plankton Research*, 20(12): 2273–2290. <https://doi.org/10.1093/plankt/20.12.2273>
- Cartes JE; Elizalde M and Sorbe J-C 2001. Contrasting life-histories, secondary production, and trophic structure of Peracarid assemblages of the bathyal suprabenthos from the Bay of Biscay (NE Atlantic) and the Catalan Sea (NW Mediterranean). *Deep-Sea Research Part I: Oceanographic Research Papers*, 48(10): 2209–2232. [https://doi.org/10.1016/S0967-0637\(01\)00012-7](https://doi.org/10.1016/S0967-0637(01)00012-7).
- Cunha MR; Sorbe J-C and Bernardes C 1997. On the structure of the neritic suprabenthic communities from the Portuguese continental margin. *Marine Ecology Progress Series*, 157: 119–137. <https://www.int-res.com/articles/meps/157/m157p119.pdf>
- Fukuoka K and Murano M 2006. Taxonomy of the genus *Meterythropros* (Crustacea: Mysida: Mysidae), with a redescription of *M. microphthalmus* and descriptions of two new species. *Journal of Natural History*, 40(27–28): 1641–1674. <https://doi.org/10.1080/00222930600956858>.
- Hansen HJ 1910. The Schizopoda of the Siboga Expedition. Siboga Expeditie, Monographie, 37: 1–77, pls. I–XII. Leyden, Brill.
- Haworth AH 1825. XXIX. A new binary arrangement of the Macrurous Crustacea. *The Philosophical Magazine and Journal, London*, 65(323): 183–184. <https://doi.org/10.1080/14786442508628417>.
- Holt EWL and Tattersall WM 1905. Schizopodous Crustacea from the north-east Atlantic Slope. Report on the sea and inland fisheries of Ireland. Part II. Scientific Investigations, Appendix IV (1902–1903): 99–152, pls. XV–XXV. Dublin, Fisheries Research Board of Ireland.
- Holt EWL and Tattersall WM 1906. Schizopodous Crustacea from the Northeast Atlantic Slope. Supplement. Report on the sea and inland fisheries of Ireland. Part II. Scientific Investigations, Appendix V (1904): 1–49, pls. I–V. Dublin, Fisheries Research Board of Ireland.
- Kou Q; Meland K; Li X; He L and Wang Y 2020. “Unicorn from Hades”, a new genus of Mysidae (Malacostraca: Mysida) from the Mariana Trench, with a systematic analysis of the deep-sea mysids. *Molecular Phylogenetics and Evolution*, 143: 106666. <https://doi.org/10.1016/j.ympev.2019.106666>.
- Lo Bianco S 1903. Le pesche abissali eseguite de F.A. Krupp col yacht Puritan nelle adiacenze di Capri ed in altre località del Mediterraneo. *Mittheilungen aus der Zoologischen Station zu Neapel*, 16(1, 2): 109–279, tav. 7–9. <https://www.biodiversitylibrary.org/item/37412#page/120/mode/1up>
- Mauchline J 1986. The biology of the deep-sea species of Mysidacea (Crustacea) of the Rockall Trough. *Journal of the Marine Biological Association of the United Kingdom*, 66(4): 803–825. <https://doi.org/10.1017/S002531540004844X>.
- Mees J and Meland K (Eds.) 2022. World List of Lophogastrida, Stygiomysida and Mysida. Accessed through: World Register of Marine Species. Instant Web Publishing. <https://doi.org/10.14284/170>.
- Meland K and Willassen E 2004. Molecular phylogeny and biogeography of the genus *Pseudomma* (Peracarida: Mysida). *Journal of Crustacean Biology*, 24(4): 541–557. <https://doi.org/10.1651/C-2481>
- Meland K and Willassen E 2007. The disunity of “Mysidacea” (Crustacea). *Molecular Phylogenetics and Evolution*, 44(3): 1083–1104. <https://doi.org/10.1016/j.ympev.2007.02.009>.
- Murano M 1970. Systematic and ecological studies on Mysidacea collected by the bottom-net. *Journal of the oceanographical Society of Japan*, 26(3): 137–150. <https://doi.org/10.1007/BF02753888>.
- Murano M 1974. *Scolamblyops japonicus* gen. nov., sp. nov. (Mysidacea) from Suruga Bay, Japan. *Crustaceana*, 26(3): 225–228. <https://doi.org/10.1163/156854074X00604>.
- Nouvel H and Lagardère J-P 1976. Les Mysidacés du talus continental du Golfe de Gascogne. I. Tribu des Erythropini (genre *Erythropros* excepté). *Bulletin du Muséum national d'Histoire naturelle, 3e sér., no. 414, Zoologie*, 291: 1243–1324. <https://biostor.org/reference/250103>

- Petryashov VV 2009. The Biogeographical Division of the Arctic and North Atlantic by the Mysid (Crustacea: Mysidacea) Fauna. *Russian Journal of marine Biology*, 35(2): 97–116. <https://doi.org/10.1134/S1063074009020011>.
- Ríos P; Áltuna A; Frutos I; Manjón-Cabeza E; García-Guillén L; Macías-Ramírez A; Ibarrola TP; Gofas S; Taboada S; Souto J; Álvarez F; Saiz-Salinas JI; Cárdenas P; Rodríguez-Cabello C; Lourido A; Boza C; Rodríguez-Basalo A; Prado E; Abad-Uribarren A; Parra S; Sánchez F and Cristobo J 2022. Avilés Canyon System: Increasing the benthic biodiversity knowledge. *Estuarine, Coastal and Shelf Science*, 274: 107924. <https://doi.org/10.1016/j.ecss.2022.107924>
- San Vicente C 2017. Geographical and bathymetric distribution of mysids (Crustacea: Mysida) in the seas of the Iberian Peninsula. *Zootaxa*, 4244(2): 151–194. <https://doi.org/10.11646/zootaxa.4244.2>.
- Sars GO 1870. Nye Dybvandskrustaceer fra Lofoten. *Forhandlinger i Videnskabs-Selskabet i Christiania*, 1869: 147–174. <https://www.biodiversitylibrary.org/item/148430#page/152/mode/1up>
- Sars GO 1883. Preliminary notices on the Schizopoda of H. M. S. Challenger expedition. *Forhandlinger i Videnskabs-Selskabet*, 7: 1–43. <https://www.vliz.be/imisdocs/publications/ocrd/221162.pdf>
- Tattersall WM 1909. The Schizopoda collected by the Maia and Puritan in the Mediterranean. *Mittheilungen aus der Zoologischen Station zu Neapel*, 19(2): 117–143, Taf. 7. <https://www.biodiversitylibrary.org/item/182419#page/133/mode/1up>
- Tattersall WM 1951. A review of the Mysidacea of the United States National Museum. *Bulletin of the United States National Museum*, 201: 1–292. <https://doi.org/10.5962/bhl.part.16843>.
- Tattersall WM and Tattersall OS 1951. The British Mysidacea. Ray Society, Monograph no. 136: 1–460. London, The Ray Society.
- Wittmann KJ 2020. Lophogastrida and Mysida (Crustacea) of the “DIVA-1” deep-sea expedition to the Angola Basin (SE-Atlantic). *European Journal of Taxonomy*, 628: 1–43. <https://doi.org/10.5852/ejt.2020.628>.
- Wittmann KJ and Chevaldonné P 2021. First report of the order Mysida (Crustacea) in Antarctic marine ice caves, with description of a new species of *Pseudomma* and investigations on the taxonomy, morphology and life habits of *Mysidetes* species. *ZooKeys*, 1079: 145–227, suppl. 1. <https://doi.org/10.3897/zookeys.1079.76412>.
- Wittmann KJ; Ariani AP and Lagardère J-P 2014. Chapter 54. Orders Lophogastrida Boas, 1883, Stygiomysida Tchindonova, 1981, and Mysida Boas, 1883 (also known collectively as Mysidacea). p. 404–406. In: Vaupel Klein JC von; Charmantier-Daures M and Schram FR (Eds.), *Treatise on Zoology - Anatomy, Taxonomy, Biology. The Crustacea*. Revised and updated, as well as extended from the *Traité de Zoologie*, Vol. 4 Part B: 189–396, color plates. Brill NV, Leiden. https://doi.org/10.1163/9789004264939_006.
- Zimmer C 1909. VI. Die nordischen Schizopoden. In: Brandt K and Apstein C (Eds.), *Nordisches Plankton*, 6(1–11): 1–178. Kiel und Leipzig, Lipsius und Tischler. <https://doi.org/10.5962/bhl.title.10255>

ADDITIONAL INFORMATION AND DECLARATIONS

Author Contributions

Entire publication (100%).

Consent for publication

Given.

Competing interests

None.

Data availability

Unlimited.

Funding and grant disclosures

No funds and no grants.

Study association

No particular study defined.

Study permits

No relevant.